Supporting Information

Taylor et al. 10.1073/pnas.1207514109

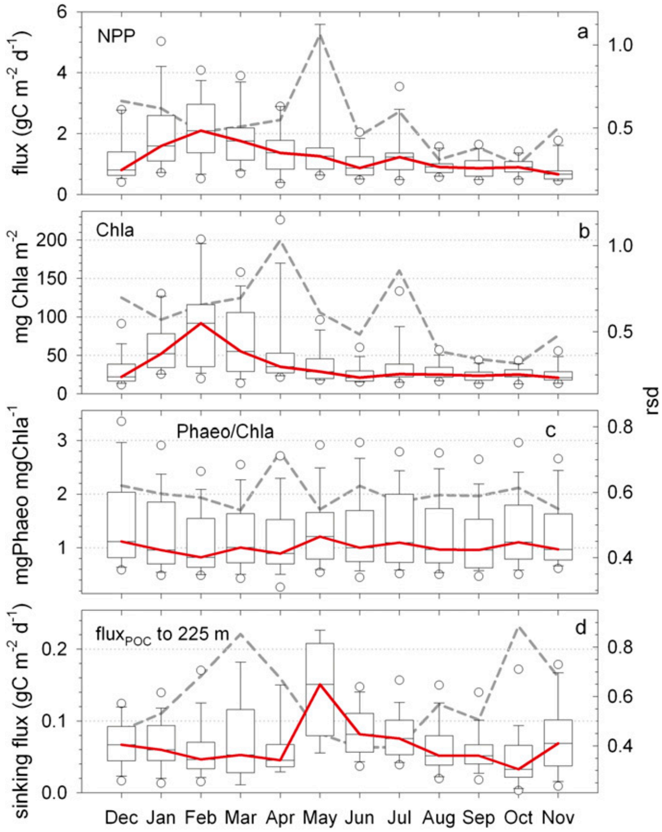

Fig. S1. Box and whisker plots depicting variations in mean annual cycles of net primary production (NPP) (*A*), Chl*a* concentrations (*B*), *phaeo*:Chl*a* ratios (*C*), and vertical flux of POC to sediment trap deployed at 225 m (*D*). Boxes represent the interquartile ranges of all observations (25th to 75th percentiles). Internal horizontal lines, whiskers, and open circles are medians, 10th to 90th, and 5th to 95th percentiles, respectively. Red curves connect medians and broken gray curves represent relative SDs (rsd = SD/mean) computed for each month among all years (n = 13–14 y).

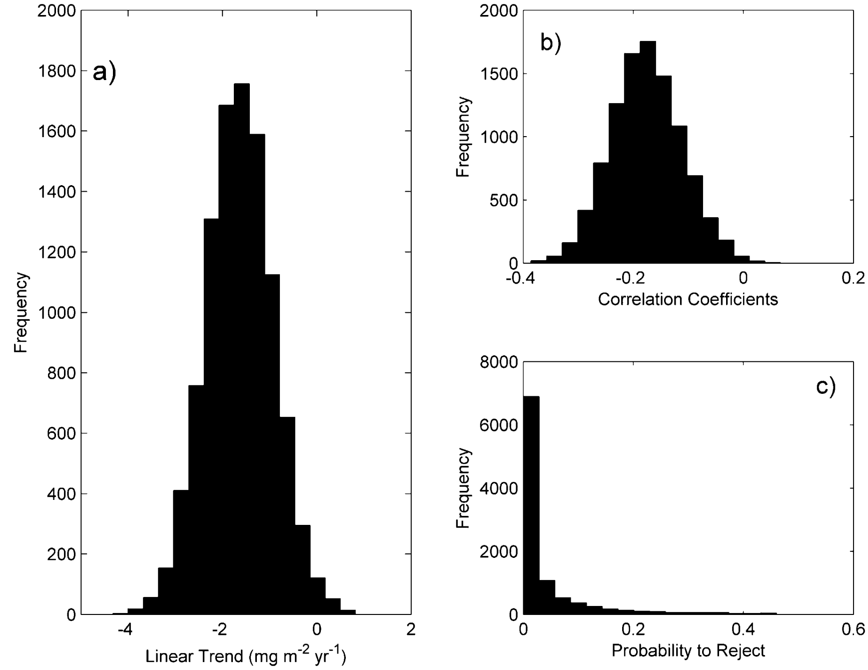

Fig. S2. Bootstrap resampling of Chl*a* anomalies. (*A*) Consensus of most reasonable estimate for Chl*a* rate of decline after 10,000 resamplings. Mode equals $-1.63\ mg{\cdot}m^{-2}{\cdot}y^{-1}$ and is essentially equivalent to regression results (Fig. 2*B* and Table 1). (*B*) Rank correlations between 9,960 Chl*a* resamplings and their time rank were negative, i.e., 99.6%. (*C*) Distribution of probabilities to reject the hypothesis that Chl*a* trend is zero. In other words, the probability that the trend is not negative is <<5%. Bootstrap resampling was performed within Statistics Toolbox of MATLAB version 2006a.

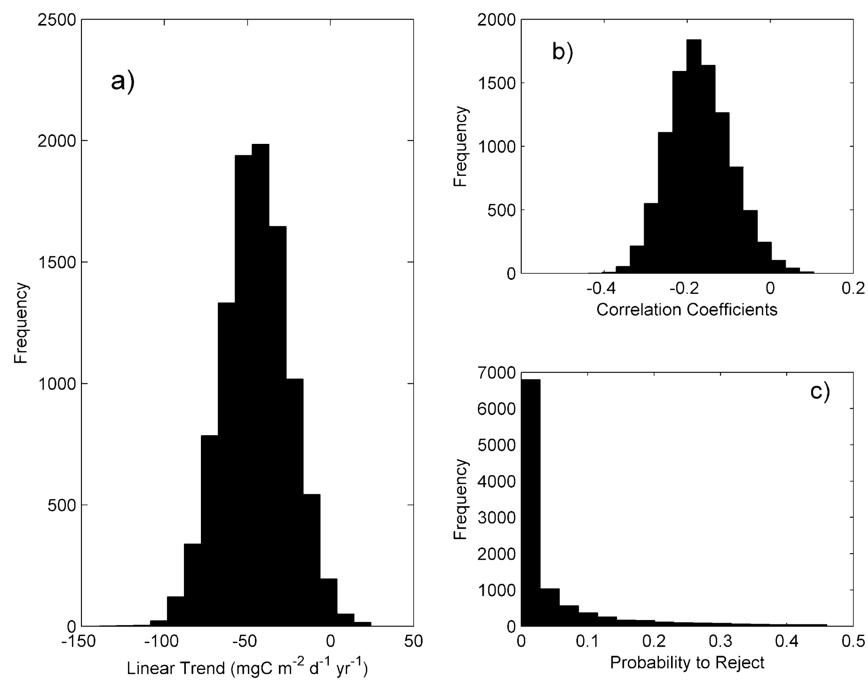

Fig. S3. Bootstrap resampling of NPP anomalies. (*A*) Consensus of most reasonable estimate for NPP rate of decline after 10,000 resamplings. Mode equals $-44\ mg\ C{\cdot}m^{-2}{\cdot}d^{-1}{\cdot}y^{-1}$ and is within the error of regression results (Fig. 2*C* and Table 1). (*B*) Rank correlations between 9,884 NPP resamplings and their time rank were negative, i.e., 98.8%. (*C*) Distribution of probabilities to reject the hypothesis that NPP trend is zero. Probability that the trend is not negative is <<5%.

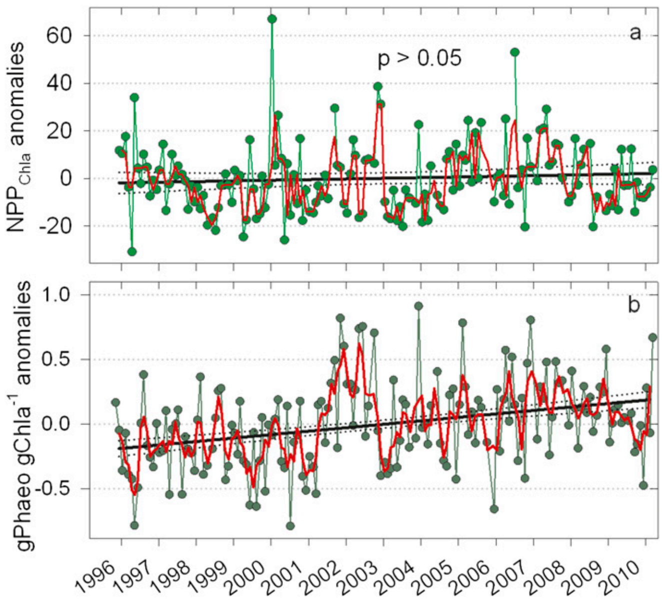

Fig. S4. Times-series of deseasonalized monthly depth-weighted means of Chl*a*-normalized net primary production (NPP_{Chla}) within the upper 100 m (*A*) and seasonally detrended, monthly depth-weighted averages of phaeopigment:chlorophyll *a* ratios (*phaeo*:Chl*a*) within the upper 100 m (*B*). Red line is three-point running trimmed means (trimean = [minimum + maximum + (2 × median)]/4) used to reduce regression sensitivity to outliers. Dotted lines enveloping slopes are 95% confidence intervals.

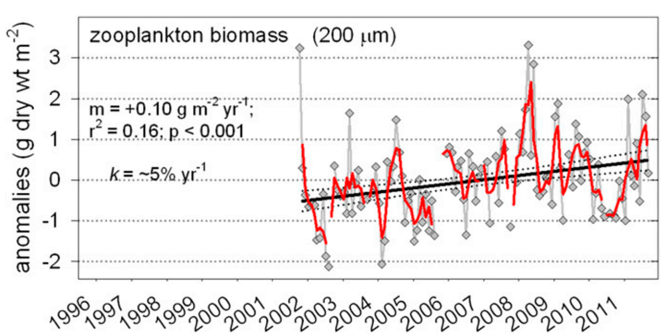

Fig. S5. Time-series of deseasonalized monthly inventories of mesozooplankton biomass (>200 μm) captured by oblique tows of paired 200- and 500-μm bongo nets (diameter, 60 cm). Earlier data are missing because monthly zooplankton sampling only commenced in October 2001. Red line is three-point running trimeans used for regression analysis. Dotted lines enveloping slopes are 95% confidence intervals. Note that first-order rates for larger zooplankton (>500 μm) were nearly equivalent; $k = 5.6\% \cdot y^{-1}$.

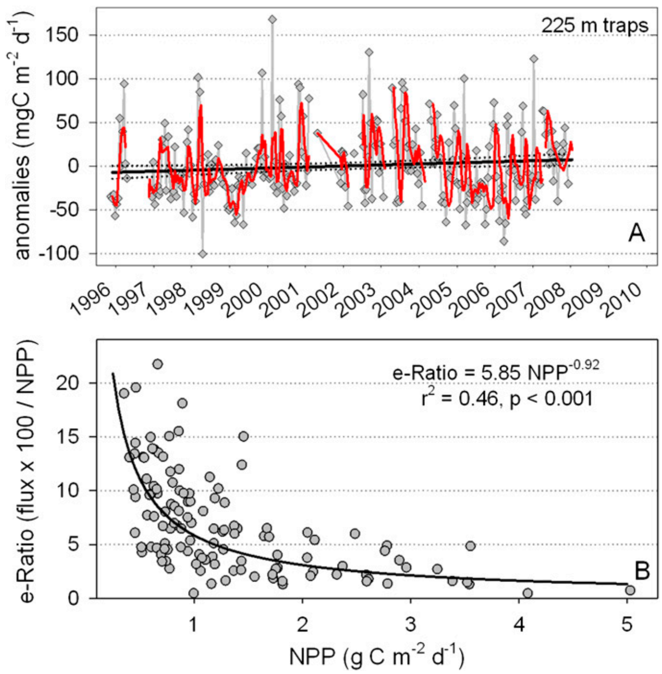

Fig. S6. Time-series of deseasonalized biweekly sinking fluxes of POC captured in moored sediment trap deployed at 225 m (*A*) and the fluxes' relationship to NPP (*B*). e-Ratio is defined here as 100 × POC fluxes to 255 m divided by contemporaneous NPP. Biweekly flux values were interpolated to temporally coincide with NPP measurements. Red line is three-point running trimeans used for regression analysis. Dotted lines enveloping slopes are 95% confidence intervals.

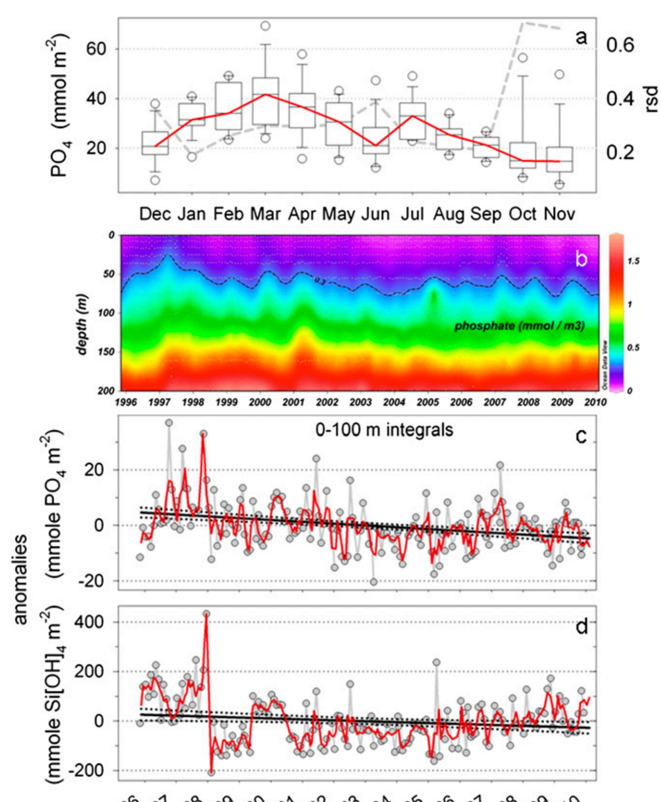

Fig. S7. Annual cycle in integrated dissolved inorganic phosphate inventories (0–100 m) (*A*), time-series of dissolved inorganic phosphate distributions in upper 200 m (*B*), deseasonalized integrated dissolved phosphate inventories in upper 100 m (*C*), and deseasonalized integrated dissolved silicate inventories (0–100 m) (*D*). (*A*) Boxes, whiskers, and open circles represent same metrics as defined in Fig. S1. Broken gray line represents the relative SD for each month. (*C* and *D*) Red lines are three-point running trimeans used for regression analysis. Dotted lines enveloping slopes are 95% confidence intervals.

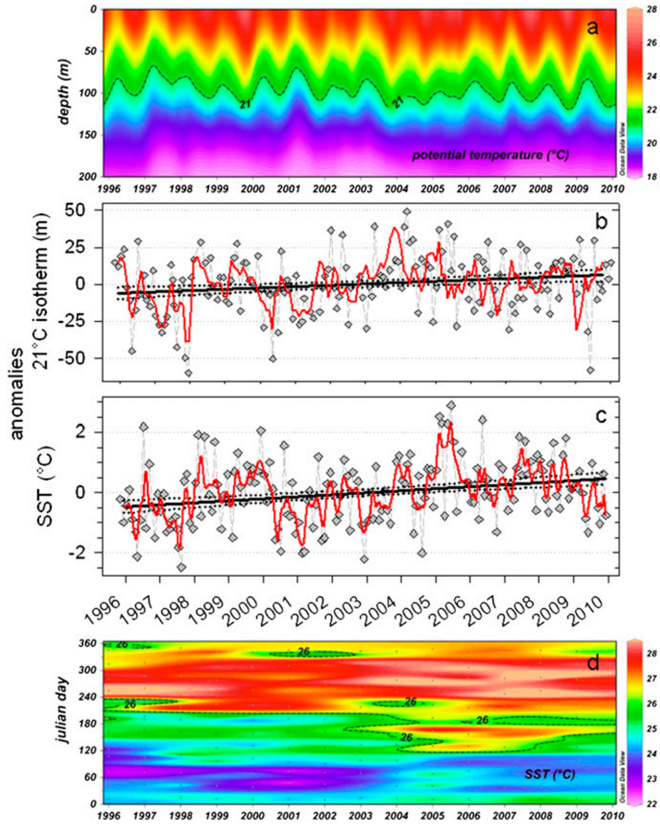

Fig. S8. Time-series of potential temperature distributions in upper 200 m (*A*), deseasonalized (anomalies) in depth of the 21 °C isotherm (*B*), anomalies in monthly SST data (*C*), and climatology of SST (*D*) over 14-y record illustrating changing seasonal pattern. Red line is three-point running trimeans used for regression analysis. Dotted lines enveloping slopes are 95% confidence intervals.

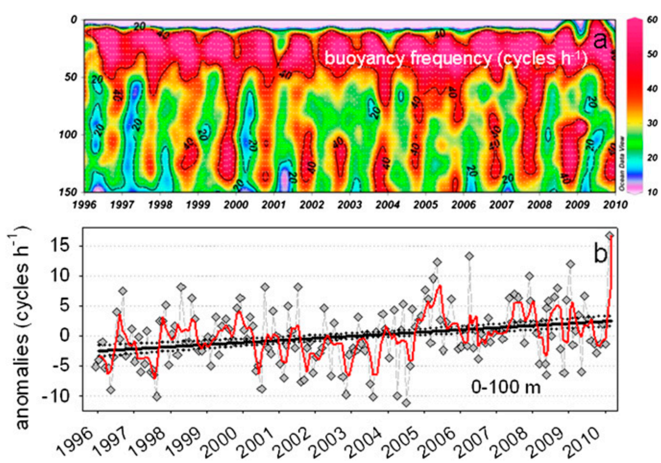

Fig. S9. Time-series of computed Brunt–Väisälä buoyancy frequencies (water column stability index) in the upper 150 m based on temperature and salinity measured at depths depicted by dots on plot (*A*) and deseasonalized monthly mean buoyancy frequency in the upper 100 m (*B*). Red line is three-point running trimeans used for regression analysis. Dotted lines enveloping slopes are 95% confidence intervals.

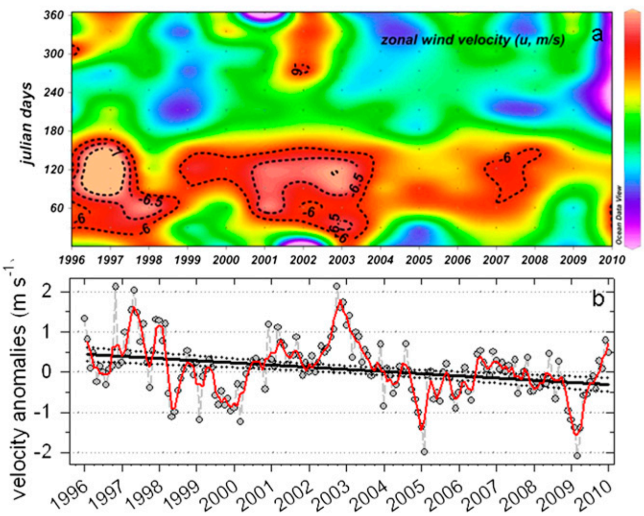

Fig. S10. Temporal variations in upwelling-favorable zonal wind velocities ($-u$) presented as monthly means of meteorological station velocity and direction measurements on Margarita Island, Venezuela. (*A*) Climatology of u over 15-y record illustrating changing seasonal pattern (negative u values indicate easterlies). (*B*) Time-series of deseasonalized monthly mean wind speeds. Red line in *B* is three-point running trimeans used for regression analysis. Dotted lines enveloping slopes are 95% confidence intervals.

Table S1. Relationship of e-Ratio to time, meteorological, hydrographic, and biotic variables as determined by linear regression analyses

Variable	Equation	r^2	*P*	*n*
Zonal winds ($m \cdot s^{-1}$)	ns	ns	ns	121
21 °C isotherm depth (m)	e-Ratio = 3.2 + 0.04 $Z_{21\ °C}$	0.06	<0.01	116
Brunt–Väisälä stability (cycles/h)	e-Ratio = 0.7 + 0.18 stability	0.06	<0.01	119
PO_4^{3-} ($mmol \cdot m^{-2}$)	e-Ratio = 11–0.13 PO_4^{3-}	0.10	<0.001	116
$Si[OH]_4$ ($mmol \cdot m^{-2}$)	e-Ratio = 10–0.012 Si	0.08	<0.005	117
NPP (mg $C \cdot m^{-2} \cdot d^{-1}$)	e-Ratio = 5.8 $NPP^{-0.92}$	0.46	<0.001	123

e-Ratio is defined here as: (POC captured in 225 m of sediment trap ÷ net primary productivity) × 100. ns, not significant (*P* value > 0.05).

Table S2. Bivariate Pearson correlation matrix of deseasonalized trends among locally observed surface ocean conditions at the CARIACO time-series station based on annual averages for each year (n = 14–15 y)

	SST	Local precip	ENSO MEI-1	Upwell	Mean density (σ_θ)	Buoyancy frequency	PO_4^{3-}	NPP	Chla
Zonal wind	**−0.72**	ns	0.49	−0.48	**0.67**	**−0.80**	0.47	**0.66**	**0.60**
SST		ns	−0.50	**0.64**	**−0.89**	**0.85**	**−0.64**	**−0.56**	**−0.79**
Local precip			ns	ns	0.46	ns	ns	ns	ns
ENSO MEI-1				ns	0.52	**−0.54**	ns	**0.60**	**0.54**
Upwell					**−0.67**	ns	**−0.90**	**−0.58**	ns
Mean density (σ_θ)						**−0.82**	**0.69**	**0.56**	**0.57**
Buoyancy frequency							ns	**−0.56**	**−0.72**
PO_4^{3-}								**0.64**	ns
NPP									**0.65**

Statistical significance levels are specified as follows: >90%, >95% (bold), >99% (bold-underline); and <90% (ns, not significant). Analysis was performed on annual means of monthly departures (1996–2009) from long-term means (anomalies). Buoyancy frequency (Brunt–Väisälä), mean level of stratification in upper 100 m (cycles/h); Chla, integrated chlorophyll *a* biomass (mg $Chla \cdot m^{-2}$); ENSO MEI-1, lagged 1 y behind multivariate ENSO index; local precip, monthly rainfall on Margarita Island (mm); mean density (σ_θ), $kg \cdot m^{-3}$ in upper 100 m; NPP, integrated net primary productivity (g $C \cdot m^{-2} \cdot d^{-1}$); PO_4^{3-}, integrated dissolved phosphate inventories in upper 100 m (mol $PO_4^{3-} \cdot m^{-2}$); SST, SST in upper 4 m (°C); upwell, depth of the 21 °C isotherm (m); zonal wind, monthly average $-u$ ($m \cdot s^{-1}$ of easterly winds).

Table S3. Bivariate Pearson correlation matrix of deseasonalized trends among basin-scale atmospheric climatological indices and locally observed surface ocean conditions at the CARIACO time-series station based on average annual anomalies for each year (*n* = 14–15 y)

	Azores SLP	Azores long	Azores lat	ITCZ precip	ITCZ long	ITCZ lat	ENSO MEI	ENSO MEI-1	Zonal wind	Upwell	SST	Local precip
NAO index	**0.74**	ns	ns	ns	ns	ns	ns	**−0.64**	ns	ns	0.51	ns
Azores SLP		ns	ns	0.50	ns	ns	ns	−0.50	0.50	ns	ns	ns
Azores long			0.47	ns	−0.49	ns	ns	ns	ns	ns	ns	ns
Azores lat				ns	ns	ns	ns	ns	ns	**0.60**	**0.75**	ns
ITCZ precip					ns	ns	ns	ns	ns	ns	ns	ns
ITCZ long						ns	**−0.75**	ns	−0.52	ns	ns	**−0.65**
ITCZ lat							ns	ns	ns	ns	ns	ns
ENSO MEI								ns	0.45	ns	ns	**0.93**
ENSO MEI-1									0.49	ns	**−0.50**	ns
Zonal wind										−0.48	**−0.72**	ns
Upwell											**0.64**	ns
SST												ns

Statistical significance levels specified as follows: >90%, >95% (bold), >99% (bold-underline); and <90% (ns, not significant). Analysis was performed on annual means of monthly departures (1996–2009) from long-term means (anomalies). Azores long and lat, COA position in °E longitude and °N latitude, respectively; Azores SLP, SLP at high pressure COA; ENSO MEI, monthly multivariate ENSO index; ENSO MEI-1, lagged 1 y behind MEI; ITCZ long and lat, COA position over South America in °E longitude and °N latitude, respectively; ITCZ precip, rainfall in ITCZ over South America; local precip, monthly rainfall on Margarita Island (mm); NAO index, differential in sea level atmospheric pressures at the Azores High and Icelandic Low; SST, SST in upper 4 m (°C); upwell, depth of the 21 °C isotherm (m); zonal wind, monthly average $-u$ ($m \cdot s^{-1}$ of easterly winds).